DR. DANIELE COSTANTINI (Orcid ID : 0000-0001-7438-4578)

Article type : Original

Modulation of biliary cancer chemo-resistance through microRNA-mediated rewiring of the expansion of CD133+ cells

Short title: MIR1249 as mediator of chemo-resistance in cholangiocarcinoma (CCA)

Pietro Carotenuto[1-2], Somaieh Hedayat[3], Matteo Fassan[4], Vincenzo Cardinale[5], Andrea Lampis[3], Vincenza Guzzardo[4], Caterina Vicentini[6], Aldo Scarpa[6], Luciano Cascione[7], Daniele Costantini[5], Guido Carpino[8], Domenico Alvaro[9], Michele Ghidini[1-10], Francesco Trevisani[3], Robert Te Poele[1], Massimiliano Salati[1], Sofia Ventura[1], Georgios Vlachogiannis[3], Jens C Hahne[3], Luke Boulter[11], Stuart J Forbes[12], Rachel Guest[12], Umberto Cillo[4], Ian Said-Huntingford[3], Ruwaida Begum[13], Elizabeth Smyth[13], Vasiliki Michalarea[13], David Cunningham[13], Lorenza Rimassa[10-14], Armando Santoro[10-14], Massimo Roncalli[15], Vladimir Kirnkin[1], Paul Clarke[1], Paul Workman[1], Nicola Valeri[3,13], Chiara Braconi[1,13,16*]

[1] Division of Cancer Therapeutics, Institute of Cancer Research, SM2 5NG, London, UK;
[2] Telethon Institute of Genetics and Medicine, Via Campi Flegrei 34, 80078 Pozzuoli (NA), Italy
[3] Division of Molecular Pathology, Institute of Cancer Research, SM2 5NG, London, UK;
[4] Department of Medicine, Surgical Pathology Unit, University of Padua, 35139, Padua, IT;
[5] Department of Medico-Surgical Sciences and Biotechnologies, Sapienza University of Rome, Latina, 04100, IT
[6] Department of Pathology, University of Verona, 37126, Verona, IT;
[7] Bioinformatics Core Unit, Institute of Oncology Research, 6500, Bellinzona, CH;
[8] Department of Movement, Human and Health Sciences, University of Rome Foro Italico, Rome, 00135, IT

[9] Department of Translational and Precision Medicine, Sapienza University, 00185, Rome, IT;
[10] Medical Oncology and Hematology Unit, Humanitas Cancer Center, Humanitas Clinical and Research Center-IRCCS, 20089, Rozzano, IT
[11] MRC Human Genetics Unit, Institute of Genetics and Molecular Medicine, EH4 2XU. Edinburgh, UK;
[12] Centre for Regenerative Medicine, University of Edinburgh, EH16 4UU. Edinburgh, UK;
[13] The Royal Marsden NHS Trust Surrey and London, SM2 5TP, Sutton, UK;
[14] Department of Biomedical Sciences, Humanitas University, 20089, Rozzano, IT
[15] Department of Pathology, Humanitas Research Hospital & Hunimed University, Rozzano (Milan) Italy
[16] The Institute of Cancer Sciences, University of Glasgow, G61 1QH, Glasgow, UK

[*]**Corresponding and lead author:** Chiara Braconi, The Institute of Cancer Science, University of Glasgow, Glasgow, UK, G61 1QH. Phone: +44(0) 141 3303278. Fax: 0141 942 6521 Email: chiara.braconi@glasgow.ac.uk

Keywords: MIR1249, Cholangiocarcinoma, chemotherapy, FZD8, Cancer Stem Cell.

ABSTRACT

Background and aims. Changes in single microRNA (MIR) expression have been associated with chemo-resistance in Biliary Tract Cancer (BTC). However, a global assessment of the dynamic role of the microRNome has never been performed to identify potential therapeutic targets that are functionally relevant in the BTC cell response to chemotherapy.

Approach and Results. high-throughput-screening of 997 LNA-MIR-inhibitors was performed in 6 CCA cell lines treated with Cisplatin-Gemcitabine (CG) seeking changes in cell viability. Validation experiments were performed with miRvana probes. MIR and gene expression was assessed by TaqMan-assay, RNA-sequencing and in-situ-hybridization in 4 indepedent cohorts of human BTC. Knock-out of microRNA was achieved by CRISPR-CAS9 in CCLP cells (MIR1249KO) and tested for effects on chemotherapy sensitivity *in-vitro* and *in-vivo*.

High-throughput-screening revealed that MIR1249-inhibition enhanced chemotherapy sensitivity across all cell lines. MIR1249 expression was increased in 41% of cases in human BTC. In validation experiments, MIR1249-inhibition did not alter cell viability in untreated or DMSO-treated cells; however it did increase CG effect. MIR1249 expression was increased in CD133+ biliary

cancer cells freshly isolated from the stem niche of human BTC, as well as in CD133+ chemo-resistant CCLP cells. MIR1249 modulated the chemotherapy-induced enrichment of CD133+ cells by controlling their clonal expansion via the Wnt-regulator FZD8. MIR1249KO cells had impaired expansion of the CD133+ subclone and its enrichment after chemotherapy, reduced expression of Cancer-Stem-Cell markers, and increased chemosensitivity. MIR1249KO xenograft BTC models showed tumour shrinkage after exposure to weekly CG, while WT models showed only stable disease over treatment.

Conclusions. MIR1249 mediates resistance to CG in BTC and may be tested as a novel target for therapeutics.

Introduction

Biliary tract cancers (BTC) include cholangiocarcinoma (CCA) and gallbladder cancer (GBC) and their incidence is increasing worldwide (1-4). Lack of effective radical treatments and rapid failure of palliative ones highlight the need for a better understanding of BTC biology and mechanisms of response to treatment (2, 5). Eighty-percent of BTC patients present at an advanced stage, when treatment options are limited to chemotherapy with cisplatin and gemcitabine (CG)(5). Only 11% of patients gain a long-term benefit from chemotherapy, while primary resistance is detected in 20% of patients (6). Most patients develop secondary resistance after an initial response or stabilization of the disease, which is responsible for a global median overall survival shorter than 12 months. Several mechanisms of chemo-resistance may act synergistically and drive cancer cells to escape biochemical inhibition or cell death caused by chemotherapy (7). Acquisition of stemness features in cancer cells appears to be a driver of resistance that is common with other tumour types (8, 9).

MicroRNAs (miRNA) are small non-coding-RNAs controlling mRNA expression (10). We and others demonstrated that miRNAs are aberrantly expressed in BTC and promote biliary carcinogenesis (11-19). Despite growing evidence that links single miRNAs with chemo-resistance, no comprehensive genome-wide approach has been undertaken to date to assess the functional role of miRNAs in the cellular dynamics involved in drug response in BTC. It is known that chemo-resistant is a peculiar feature of BTC that is responsible for the poor prognosis of these patients. Thus, in these studies we have investigated the functional role of microRNA inhibitors in mediating drug response in chemotherapy-treated BTC cells, using a highthroughput approach that investigates the inducible role of miRNAs in response to cancer drugs.

Experimental porcedures

Human tissues. The human BTC tissues were collected under approval of the Ethical Committee for Clinical Research at 3 independent Institutions, the Humanitas Research Hospital (#21072014; cohort 1), the Royal Marsden hospital (RMH) (CCR 4415; cohort 2), and the University Hospital of Padua (#0010416; cohort 3). The study protocols conformed to the ethical guidelines of the 1975 Declaration of Helsinki, as per ethical approval given by Institutional Review Board. Formalin Fixed Paraffin Embedded (FFPE) tissues were retrieved and RNA was extracted from the tumour and the matched non tumour component after microscopic dissection by using the Ambion RecoverAll kit (Thermofisher Waltham, Massachusetts, USA). Relapse-Free Survival (RFS) was used as end point of the study. Disease recurrence was defined as the presence of imaging-proven disease.

Highthroughput-screening (HTS). A human LNA microRNA inhibitor library (miRCURY LNA, version 3; #190102-3) was purchased from Exiqon (Life Technologies, Paisley, UK). The library was distributed across 15 x 96-well plates (Greiner Bio-One, Frickenhausen, Germany) in a volume of 5 ul each well. Each plate included two negative controls (LNA negative A, LNA negative B from Exiqon) and positive controls (AllStars-Hs-Positive cell death phenotype control, SI04381048 from Qiagen, Manchester, UK). Fifteen ul of transfecting solution with medium and Hiperfect (PN301705, Qiagen, Manchester, UK) was added to each well. Thirty µl of cell solution was then added to each well to have a final concentration of 10,000 cells and 50nM of miRNA inhibitors. A column with no cells (x 8) was added in one plate. Forty-eight hours later, 50 ul of a combination of cisplatin (C) (232120, Sigma-Aldrich, Gillingham, UK) and gemcitabine (G) (1288463-200MG, Sigma-Aldrich, Gillingham, UK) diluted in media were added. Cisplatin was dissolved in sterile PBS and stocked at a concentration of 1 mg/ml (3mM). Gemcitabine was diluted in DMSO and stocked at a concentration of 10mg/ml (30mM). Both stocks would then be diluted in media to achieve a final solution that would always contain less than 0.001% of DMSO. Cell viability was measured 72 hours later by CellTiter-Blue® Assay (Promega, Madison, WI, USA). The cell viability measurement from each hit was normalized to that of the averaged negative controls across the respective plate. Each cell line was tested in triplicate. Statistical significance ($p<=0.05$) was determined by two-sided t-test across 3 replicates.

MIR1249-KO generation through CRISPR-CAS9. CCLP-1 cells were transfected by using Lipofectamine 3000 reagent (Thermofisher, Waltham, MA, USA) with the CRISPR vector pCAS-Guide-EF1a-GFP CRISPR Vector (GE100018, OriGene Technologies, Inc. MD USA) expressing gRNAs containing the inserted target sequence for miR1249. Target sequences of the gRNA were as follows: gRNA3 5' CGTCGGTCGTGGTAGATAGG 3'; gRNA4 5'

AATCTCGACCGGACCTCGAC 3'). Forty-eight hours later GFP positive cells were sorted with a FACSAria-II (BD Biosciences, San Jose, CA, USA) and maintained in culture. Genome editing was verified at day 17 using the Indel identification kit (Clontech Biotec., Mountain View, CA, USA). Cells were enriched for the edited clones by performing serial dilution. Final assessment of the successful genome editing was performed by sequencing and real time PCR.

Statistical analyses. Statistical analyses were performed by GraphPad Prism 6 (La Jolla, CA, USA). Results are expressed as mean ± SD, unless indicated otherwise. Groups were compared with either a 2-tailed Student's *t* test (for analysis of 2 groups) or using 1-way ANOVA to compare multiple groups. Significance was accepted when *p* was less than 0.05.

Results

Highthroughput functional studies and characterization of human cancer tissues identified MIR1249 inhibition as a clinically relevant strategy to increase chemo-sensitivity in human BTC. Highthroughput screening (HTS) technologies were applied to screen a panel of 6 CG-treated BTC cell lines against a library of Locked-Nucleic-Acid (LNA) miRNA inhibitors. Growth Inhibitory (GI)50 concentration for cisplatin and gemcitabine was derived for each cell line to define the concentration at which the combination of CG could induce cytotoxicity without reducing cell viability by more than 50%, in order to enable identification of sensitizers (Suppl Figure 1). HTS was run in triplicate in each cell line (Suppl Table 1). Inhibition of MIR148a and members of the let-7 family reduced sensitivity in a number of cell lines, in line with published literature (13, 20). Eleven miRNA-inhibitors acted as sensitizers in all intrahepatic CCA (iCCA) cells, while 4 in all extrahepatic CCA (eCCA) cells ($p<0.05$) (Figure 1A). Inhibitors of MIR1249, MIR133b, MIR1247 and MIR1228 decreased cell viability across all cell lines in comparison to CTRL inhibitors. The tissue expression of these four shortlisted miRNAs was determined in human BTCs by Taqman assay to investigate the clinical relevance of these candidates. MIR133b, MIR1247 and MIR1228 expression was not increased in the tumour tissue in comparison to matched adjacent non tumour tissue (Cohort 1, n=29) (Suppl Figure 2A). Conversely, MIR1249 was over-expressed in the tumour compartment in comparison to paired non tumour tissue in 32% of cases (Figure 1B). Interestingly, when the cohort was split according to median MIR1249 tumour expression, cases with high expression were associated with worse prognosis independently of adjuvant chemotherapy (Figure 1C, Suppl Table 2). At multivariate analysis (considering T stage, N stage, adjuvant chemotherapy and MIR1249 tumour expression) adjuvant treatment (HR 0.70; $p<0.001$) and MIR1249 expression (HR 0.65; p: 0.004) maintained an independent prognostic value. An increase of MIR1249 expression by Taqman assay was

observed in 53% of cases of a separate cohort (cohort 2, n=28) (Suppl Figure 2B). When cohort 1 and 2 were pooled together 41% of cases showed increased MIR1249 expression in the tumour. RNA-sequencing data confirmed over-expression of MIR1249 in the tumour tissue in comparison to paired normal tissue in 55% of cases (TCGA cohort (21), n=9) (Suppl Figure 2C). Kaplan Meier analysis of the whole TCGA cohort showed that tumour MIR1249 expression was again associated to progression free interval (PFI) (Suppl Figure 2D). When assessed by *in situ* hybridization, MIR1249 was strongly positive in 53% of tumour cases and was statistically associated with lower survival outcome (cohort 3, n= 28) (Figure 1D-E, Suppl Table 3).

Validation functional studies identified the involvement of MIR1249 in driving a chemotherapy-specific reactive response in cancer cells. On the basis of the clinical and biological relevance of these data, MIR1249 was selected as a candidate for further studies. MIR1250 inhibitor (that provided no effect in any of the cells in the HTS) was included in the validation phase as a negative control, along with scrambled control (Suppl Figure 2E). Using alternative probes for miRNA inhibition, the ability of MIR1249 inhibitor to enhance BTC cell response to CG chemotherapy was validated. Interestingly, we did not observe a cytotoxic effect for MIR1249 inhibitor in absence of chemotherapy treatment (Figure 2), suggesting that MIR1249 interferes with a chemotherapy-specific response. Indeed, MIR1249 expression was increased as a response to CG treatment in human CCA cells (Suppl Figure 2F). Enrichment of resistant cells expressing stem cell markers is known to occur in response to chemotherapy treatment in a variety of cancers (22, 23). Thus, we hypothesized that MIR1249 inhibition can increase chemo-sensitivity by limiting the expansion of this resistant sub-population. In order to verify our hypothesis, we assessed the expression of MIR1249 in human BTC spheroids generated from human cells freshly extracted from the stem niche of BTC samples, before and after selection for surface cell markers (Figure 3A). MIR1249 expression was increased in BTC cells compared to non-cancer biliary tract stem cells (BTSC). CD133+ and CD13+ cells had increased expression of MIR1249 compared to CD133- and CD13- cells (Figure 3A). CD133 has been consistently reported to be a marker of chemo-resistant cancer cells which are enriched after treatment (22-27), and CD133+ BTC cells were shown to be tumorigenic and express features of cancer stem cells (9, 28). Therefore, we speculated that MIR1249 could affect chemo-resistance by inducing the expansion of CD133+ BTC cells. Indeed, an association between CD133 positivity and MIR1249 strong expression was observed in human BTC tissues (Suppl Figure 2G). Increased MIR1249 expression was confirmed in CCLP-1 CD133+ cells sorted from 2D cultures both by Taqman assays and ISH (Figure 3B). CD133+ cells gave rise to spheroids, indicating their self-renewal properties (Figure 3B-C) and were more resistant to CG chemotherapy, when cultured in

2D (Suppl Figure 2H) or 3D (Figure 3C&D), in comparison to CD133- cells. Inhibition of MIR1249 in CD133+ CCLP-1 cells increased sensitivity in comparison to CTRL microRNA inhibitor, while MIR1249 enforced expression in CD133- cells reduced sensitivity to CG chemotherapy (Figure 4A, Suppl Figure 2I). In order to understand the potential of MIR1249 to control the expansion of CD133+ cells, we studied the fraction of CD133+ cells in the presence and absence of MIR1249 modulation. Enforced expression of MIR1249 in BTC cells expanded the proportion of CD133+ sub-population (Figure 4B), which had increased expression of stem cell markers (Figure 4C). Indeed, CSC markers were increased in CD133+ vs CD133- cells, and after transfection with MIR1249 mimic compared to mimic control (Figure 4C). Conversely, inhibition of MIR1249 reduced the CG-induced enrichment of CD133+ cells (Figure 4D). To confirm the role of MIR1249 in the expansion of CD133+ cells, we generated a MIR1249KO CCLP-1 cell line using CRISPR-CAS9 technologies (Suppl Fig 3A&B&C). MIR1249KO cells were more sensitive to CG treatment with a concentration-response effect (Fig 4E) and showed impaired expansion of CD133+ cells (Suppl Fig 3D & Figure 4F), along with reduced expression of cancer stem cell (CSC) marker (Suppl Fig 3E) and lack of spheroid formation (Suppl Fig 3F). Reintroduction of MIR1249 in MIR1249KO cells restored chemoresistance in CCLP-1 cells (Fig 4G & Suppl Fig 3G).

MIR1249 drives clonal expansion of CD133+ cells by re-wiring the Wnt pathway activation. In order to identify the mechanisms through which MIR1249 mediates chemo-resistance, we characterized the gene expression profiles of chemotherapy-treated CCLP-1 cells after inhibition of MIR1249. Pathway analysis of the deregulated genes showed that MIR1249 inhibition induced changes in the same pathways that were deregulated by chemotherapy. We noticed an enrichment of deregulated genes in the Wnt pathway in both comparisons (chemotherapy vs vehicle; MIR1249 inhibition vs no inhibition), suggesting that MIR1249 inhibition may act on the Wnt pathway to restore chemotherapy sensitivity in BTC cells (Suppl Fig 3H&I). In line with this hypothesis, Wnt deregulation was previously found to drive proliferation of chemo-refractory CSC (29, 30). PANTHER pathway analysis of the predicted targets of MIR1249 based on DIANA software showed an enrichment of Wnt signalling (fold enrichment 1.41; p:9.1E-03). *In silico* analyses revealed, amongst others, frizzled class receptor 8 (FZD8) as a potential mRNA target of MIR1249 (Suppl Fig 3L). Previous evidence suggests that FZD8 can act as a negative regulator of the canonical Wnt pathway by activating the non-canonical Wnt/Ca^{++} signalling (31-34). Thus, we hypothesized that MIR1249 mediates the expansion of CD133+ cells by acting on FZD8. Indeed, FZD8 was significantly reduced in CD133+ in comparison to CD133- cells and was associated with inactivation of the non-canonical Wnt and activation of the canonical Wnt pathway (Fig 5A&B). FZD8 protein expression was reduced in CD133- cells transfected with

MIR1249 mimic in comparison to control (CTRL) mimic (Figure 5A), and a luciferase reporter test confirmed a direct interaction between MIR1249 and the 3'UTR of FZD8 (Figure 5C). In human BTC samples (cohort 3) there was a significant inverse relation between MIR1249 and FZD expression (Fisher exact test p:0.004; Suppl Fig 3N). Inhibition of FZD8 recapitulated the phenotype induced by MIR1249 mimic (Figure 5D&E&F). MIR1249KO cells had increased activation of the non-canonical Wnt pathway (Fig 5G&H, Suppl Fig 3M and Suppl Table 4) and FZD8 inhibition in these cells partially increased resistance to CG (Fig 5I).

In-vivo validation of the MIR1249-dependent chemo-resistance in murine tumours bearing disruption of MIR1249. MIR1249KO cells had reduced *in-vivo* tumorigenicity, confirming the role of MIR1249 in driving the expansion of CSC (Figure 6A, Suppl Fig S4A). Chemotherapy sensitivity was increased in mice bearing MIR1249KO tumour xenografts. Indeed, the weekly combination of CG could induce tumour shrinkage in MIR1249KO xenografts while determined only tumour stabilization in wild type (WT) xenografts (Figure 6B&C&D, Suppl Table 5). The chemotherapy schedule was well tolerated with only minimal changes in weights for CG-treated mice at the end of the treatment course. No differences in weights were observed between WT and MIR1249KO CG-treated mice, suggesting that the drug exposure was comparable amongst the two groups (Figure 6E). In addition, no differences in liver and kidney toxicity were observed between WT and MIR1249KO mice when treated with CG (Suppl Fig4B&C). To confirm the role of MIR1249 in driving the expansion of CD133+ cells via FZD8 we assessed protein expression in explanted tumours from MIR1249KO vs WT xenograft (either treated with CG and vehicle) and observed that MIR1249KO tumours showed lack of MIR1249 expression and reduced expression of CD133, with increase in FZD8 expression (Figure 6F).

Discussion

Therapeutic development for BTC remains an unmet need. Chemotherapy does represent the main backbone for advanced biliary cancers (ABC) treatment even though the response rate observed in ABC patients does not exceed 25%. Novel strategies aimed at improving the efficacy of chemotherapy might prove beneficial to a large proportion of ABC patients. The field of miRNA-based therapeutics has recently expanded and entered the phase of clinical investigation (10, 35, 36). The ability of miRNAs to target multiple pathways is attractive as it may prevent the onset of compensatory pathways.

Data from the MesomiR1 trial have shown the feasibility of a therapeutic approach based on miRNA replacement in human cancer patients (37). However, this approach holds two major

limitations: 1) toxicity related to the immuno-stimulatory effects of encapsulating delivery systems, and 2) off-target effects induced by a disproportionally high level of miRNA in the cellular system. Conversely, an approach based on the inhibition of miRNAs would reduce the risk of off-target effects by impacting on the physiological level of a miRNA rather than introducing a perturbation that affects cellular homeostasis. Recent technologies have enabled chemical modifications of anti-miRs (i.e. addition of LNA) that increase their stability (38), allowing the clinical investigation of this therapeutic strategy in cancer patients (NCT02580552). In these studies, we have identified MIR1249 as a miRNA that drives the emergence of chemo-resistance by acting on the CD133+ cell population. While we usually observe tumour stabilization with chemotherapy in BTC patients, our data suggest that the addition of MIR1249 inhibition to CG can increase tumour responses *in-vivo*. It is known that partial responses are associated with prolonged life expectancy in BTC patients, and therefore we speculate that treatment with MIR1249 inhibitors might prove beneficial to impact on survival of BTC patients by preventing primary resistance and delaying the onset of secondary resistance. It has been shown already that the canonical WNT/β-catenin signaling mediates self-renewal of stem cells, while non-canonical WNT signaling pathways is involved in maintenance of stem cells, cell plasticity and inhibition of the canonical WNT signaling cascade (29), supporting our data that MIR1249 can drive maintenance and expansion of CSC through regulation of the non-canonical Wnt pathway. With regards to FZD8, data in the literature are so far contradictory, with some reports showing the capacity of FZD8 to stimulate malignant transformation of cancer cells (39), and others showing its involvement in reducing tumour initiating capacity (32). In line with our data that showed low expression of FZD8 in CSC, analysis of the ATLAS datasets showed unfavorable prognosis in cases of pancreatic cancers with low FZD8 expression. Nonetheless, the attempts to therapeutically inhibit FZD8 have failed so far lack of therapeutic index, suggesting that FZD8 may not be involved in promoting cancer growth.

Last, to our knowledge, this is the first time the combination of CG has been given in a weekly schedule to BTC mouse models in an attempt to better mimic the schedule used in the ABC-02 trial which licensed the combination CG for standard clinical practice. We noticed good tolerance of this schedule and suggest that this regimen should be used in the future in *in-vivo* BTC modelling in order to increase clinical relevance of pre-clinical findings.

In conclusion, we have provided evidence for a potential target to be taken forward in the therapeutic development. From our data MIR1249 is involved in the chemotherapy resistance in all different subtypes of CCA, and therefore we would suggest testing MIR1249 inhibitor in a trial including ABC. In addition, it may be speculated that this mechanism may be shared with other cancer types as well, and therefore investigation in other solid tumours may be warranted.

REFERENCES

1. Khan SA, Emadossadaty S, Ladep NG, Thomas HC, Elliott P, Taylor-Robinson SD, Toledano MB. Rising trends in cholangiocarcinoma: is the ICD classification system misleading us? J Hepatol 2012;56:848-854.

2. Bridgewater J, Galle PR, Khan SA, Llovet JM, Park JW, Patel T, Pawlik TM, et al. Guidelines for the diagnosis and management of intrahepatic cholangiocarcinoma. J Hepatol 2014;60:1268-1289.

3. Marcano-Bonilla L, Mohamed EA, Mounajjed T, Roberts LR. Biliary tract cancers: epidemiology, molecular pathogenesis and genetic risk associations. Chin Clin Oncol 2016;5:61.

4. Saha SK, Zhu AX, Fuchs CS, Brooks GA. Forty-Year Trends in Cholangiocarcinoma Incidence in the U.S.: Intrahepatic Disease on the Rise. Oncologist 2016;21:594-599.

5. Valle J, Wasan H, Palmer DH, Cunningham D, Anthoney A, Maraveyas A, Madhusudan S, et al. Cisplatin plus gemcitabine versus gemcitabine for biliary tract cancer. N Engl J Med 2010;362:1273-1281.

6. Bridgewater J, Lopes A, Palmer D, Cunningham D, Anthoney A, Maraveyas A, Madhusudan S, et al. Quality of life, long-term survivors and long-term outcome from the ABC-02 study. Br J Cancer 2016;114:965-971.

7. Marin JJ, Briz O, Rodriguez-Macias G, Diez-Martin JL, Macias RI. Role of drug transport and metabolism in the chemoresistance of acute myeloid leukemia. Blood Rev 2016;30:55-64.

8. Ishiwata T. Cancer stem cells and epithelial-mesenchymal transition: Novel therapeutic targets for cancer. Pathol Int 2016;66:601-608.
9. Huang L, Cai J, Guo H, Gu J, Tong Y, Qiu B, Wang C, et al. ID3 Promotes Stem Cell Features and Predicts Chemotherapeutic Response of Intrahepatic Cholangiocarcinoma. Hepatology 2018.
10. Salati M, Braconi C. Noncoding RNA in Cholangiocarcinoma. Semin Liver Dis 2018.
11. Meng F, Henson R, Wehbe-Janek H, Ghoshal K, Jacob ST, Patel T. MicroRNA-21 regulates expression of the PTEN tumor suppressor gene in human hepatocellular cancer. Gastroenterology 2007;133:647-658.
12. Selaru FM, Olaru AV, Kan T, David S, Cheng Y, Mori Y, Yang J, et al. MicroRNA-21 is overexpressed in human cholangiocarcinoma and regulates programmed cell death 4 and tissue inhibitor of metalloproteinase 3. Hepatology 2009;49:1595-1601.
13. Braconi C, Huang N, Patel T. MicroRNA-dependent regulation of DNA methyltransferase-1 and tumor suppressor gene expression by interleukin-6 in human malignant cholangiocytes. Hepatology 2010;51:881-890.
14. Braconi C, Valeri N, Gasparini P, Huang N, Taccioli C, Nuovo G, Suzuki T, et al. Hepatitis C virus proteins modulate microRNA expression and chemosensitivity in malignant hepatocytes. Clin Cancer Res 2010;16:957-966.
15. Braconi C, Valeri N, Kogure T, Gasparini P, Huang N, Nuovo GJ, Terracciano L, et al. Expression and functional role of a transcribed noncoding RNA with an ultraconserved element in hepatocellular carcinoma. Proc Natl Acad Sci U S A 2011;108:786-791.
16. Carotenuto P, Fassan M, Pandolfo R, Lampis A, Vicentini C, Cascione L, Paulus-Hock V, et al. Wnt signalling modulates transcribed-ultraconserved regions in hepatobiliary cancers. Gut 2017;66:1268-1277.
17. Braconi C, Patel T. Cholangiocarcinoma: new insights into disease pathogenesis and biology. Infect Dis Clin North Am 2010;24:871-884, vii.
18. Lampis A, Carotenuto P, Vlachogiannis G, Cascione L, Hedayat S, Burke R, Clarke P, et al. MIR21 Drives Resistance to Heat Shock Protein 90 Inhibition in Cholangiocarcinoma. Gastroenterology 2018;154:1066-1079 e1065.
19. Braconi C, Roessler S, Kruk B, Lammert F, Krawczyk M, Andersen JB. Molecular perturbations in cholangiocarcinoma: Is it time for precision medicine? Liver Int 2019.

20. Meng F, Henson R, Wehbe-Janek H, Smith H, Ueno Y, Patel T. The MicroRNA let-7a modulates interleukin-6-dependent STAT-3 survival signaling in malignant human cholangiocytes. J Biol Chem 2007;282:8256-8264.

21. Farshidfar F, Zheng S, Gingras MC, Newton Y, Shih J, Robertson AG, Hinoue T, et al. Integrative Genomic Analysis of Cholangiocarcinoma Identifies Distinct IDH-Mutant Molecular Profiles. Cell Rep 2017;19:2878-2880.

22. Steg AD, Bevis KS, Katre AA, Ziebarth A, Dobbin ZC, Alvarez RD, Zhang K, et al. Stem cell pathways contribute to clinical chemoresistance in ovarian cancer. Clin Cancer Res 2012;18:869-881.

23. Auffinger B, Tobias AL, Han Y, Lee G, Guo D, Dey M, Lesniak MS, et al. Conversion of differentiated cancer cells into cancer stem-like cells in a glioblastoma model after primary chemotherapy. Cell Death Differ 2014;21:1119-1131.

24. Suetsugu A, Nagaki M, Aoki H, Motohashi T, Kunisada T, Moriwaki H. Characterization of CD133+ hepatocellular carcinoma cells as cancer stem/progenitor cells. Biochem Biophys Res Commun 2006;351:820-824.

25. Suetsugu A, Osawa Y, Nagaki M, Moriwaki H, Saji S, Bouvet M, Hoffman RM. Simultaneous color-coded imaging to distinguish cancer "stem-like" and non-stem cells in the same tumor. J Cell Biochem 2010;111:1035-1041.

26. Cortes-Dericks L, Carboni GL, Schmid RA, Karoubi G. Putative cancer stem cells in malignant pleural mesothelioma show resistance to cisplatin and pemetrexed. Int J Oncol 2010;37:437-444.

27. Kelly SE, Di Benedetto A, Greco A, Howard CM, Sollars VE, Primerano DA, Valluri JV, et al. Rapid selection and proliferation of CD133+ cells from cancer cell lines: chemotherapeutic implications. PLoS One 2010;5:e10035.

28. Cardinale V, Renzi A, Carpino G, Torrice A, Bragazzi MC, Giuliante F, DeRose AM, et al. Profiles of cancer stem cell subpopulations in cholangiocarcinomas. Am J Pathol 2015;185:1724-1739.

29. Katoh M. Canonical and non-canonical WNT signaling in cancer stem cells and their niches: Cellular heterogeneity, omics reprogramming, targeted therapy and tumor plasticity (Review). Int J Oncol 2017;51:1357-1369.

30. Mohammed MK, Shao C, Wang J, Wei Q, Wang X, Collier Z, Tang S, et al. Wnt/beta-catenin signaling plays an ever-expanding role in stem cell self-renewal, tumorigenesis and cancer chemoresistance. Genes Dis 2016;3:11-40.
31. Semenov MV, Habas R, Macdonald BT, He X. SnapShot: Noncanonical Wnt Signaling Pathways. Cell 2007;131:1378.
32. Wang MT, Holderfield M, Galeas J, Delrosario R, To MD, Balmain A, McCormick F. K-Ras Promotes Tumorigenicity through Suppression of Non-canonical Wnt Signaling. Cell 2015;163:1237-1251.
33. Sugimura R, Li L. Noncanonical Wnt signaling in vertebrate development, stem cells, and diseases. Birth Defects Res C Embryo Today 2010;90:243-256.
34. Masoumi KC, Daams R, Sime W, Siino V, Ke H, Levander F, Massoumi R. NLK-mediated phosphorylation of HDAC1 negatively regulates Wnt signaling. Mol Biol Cell 2017;28:346-355.
35. Rupaimoole R, Slack FJ. MicroRNA therapeutics: towards a new era for the management of cancer and other diseases. Nat Rev Drug Discov 2017;16:203-222.
36. Constantinescu CA, Fuior EV, Rebleanu D, Deleanu M, Simion V, Voicu G, Escriou V, et al. Targeted Transfection Using PEGylated Cationic Liposomes Directed Towards P-Selectin Increases siRNA Delivery into Activated Endothelial Cells. Pharmaceutics 2019;11.
37. van Zandwijk N, Pavlakis N, Kao SC, Linton A, Boyer MJ, Clarke S, Huynh Y, et al. Safety and activity of microRNA-loaded minicells in patients with recurrent malignant pleural mesothelioma: a first-in-man, phase 1, open-label, dose-escalation study. Lancet Oncol 2017;18:1386-1396.
38. Cheng CJ, Bahal R, Babar IA, Pincus Z, Barrera F, Liu C, Svoronos A, et al. MicroRNA silencing for cancer therapy targeted to the tumour microenvironment. Nature 2015;518:107-110.
39. Yin S, Xu L, Bonfil RD, Banerjee S, Sarkar FH, Sethi S, Reddy KB. Tumor-initiating cells and FZD8 play a major role in drug resistance in triple-negative breast cancer. Mol Cancer Ther 2013;12:491-498.

Figures legend

Figure 1. MIR1249 represents a clinically significant candidate for therapeutics based on *in-vitro* HTS data and expression profiles of human BTC samples. (A) Hightroughput screening technologies were applied to 6 cell lines in triplicate. Cells were reverse transfected with LNA miRNA inhibitors for 48 hours followed by treatment with CG chemotherapy (see also Figure S1). After 72 hours cell viability was assessed by Cell-Titer blue assay. Each square indicates logarithmic value of the mean of cell viability normalized to averaged negative controls (N=3), with color code indicating the degree of change in cell viability. Here we show miRNA inhibitors which were significant ($p<0.05$) in enhancing chemosensitivity across all iCCA or across all eCCA ($p<0.05$). * indicates miRNA inhibitors that were significant across all 6 cell lines (see also Table S1). (B) MIR1249 expression was assessed by Taqman assay in the tumour (TT) and adjacent tissue (AT) of 29 human clinically annotated BTC samples (cohort 1) (see also Table S2). Insufficient RNA quality was achieved for the AT of one case, thus data for 28 cases are shown. Bars represent mean values of 2 technical replicates for each patient. Purple, yellow and green bars indicate iCCA, eCCA and GBC respectively. (C) Kaplan Meier analysis was used to correlate relapse free survival (RFS) with MIR1249 tumour tissue expression. Cases were classified in low and high MIR1249 expression according to the median value. (D) MIR1249 expression was assessed by ISH in 28 FFPE human BTC tissues (cohort 2). Representative pictures are shown (see also Table S3). Original magnifications 10X (left) and 20X (right). (E) Kaplan Meier curves in cohort 2 with respect to MIR1249 expression (strong: ISH score 2+ or greater; neg/mild: ISH score 0 or 1+).

Figure 2. MIR1249 inhibition decreases cell viability in chemotherapy-treated cells only. (A) MIR1249 inhibition was achieved using miRvana inhibitory probes. Cells were plated in 96 well plates and transfected with the indicated probes for 48 hours before being treated with DMSO or CG for further 72 hours. Cell Death CTRL was used as a positive control. Cell viability was assessed by CellTiter blue assay. Bars indicate mean of 6 independent experiments +/- standard deviation (SD).

Figure 3. Human CD133+ BTC cells hold high MIR1249 levels and are highly chemo-resistant. (A) Cancer stem cell niche of human BTC samples was identified, cells were then extracted, sorted by cell surface markers and cultured in 3D spheroids. MIR1249 expression was assessed by Taqman assay. Bars indicate 3 independent replicates +/- SD. BTSC: Biliary Tract Stem Cells. (B) CCLP-1 cells were sorted by FACS for CD133 surface expression. MIR1249 was assessed both by Taqman (blue bars indicating mean of three independent experiments +/-SD) and by ISH (representative pictures are shown, scale bar: 100μM). (C) When cultured in ultra-low attachment plates (ULA) CD133+ cells formed large and defined 3D spheroids conversely to CD133- cells. (C) CCLP-1 cells were sorted for CD133 surface expression and cultured in ULA plates. After 5 days baseline imaging of spheroids by Celigo showed reproducible spheroid formation across the plates, even though CD133- spheroids were smaller. After 3 days of CG treatment (scalar concentrations up to 3μM cisplatin and 30nM gemcitabine) CD133- spheroids shrank in volume, while CD133+ spheroids did not, even at the highest CG concentration. Bars represent mean of 6 replicates +/- SD. (D) Representative pictures of spheroids with and without CG treatment. Spheroids were monitored up to 6 days. CD133- spheroids volume reduced from baseline, while CD133+ spheroids volume was stabilized (see also Figure S2).

Figure 4. MIR1249 inhibition prevents chemotherapy-induced enrichment of CD133+ sub-clone. (A) CCLP-1 cells were transfected with indicated probes after being sorted for CD133 surface expression. Mock indicates absence of any probe. Chemotherapy was added 48 hours after transfection, and cell viability read 72 hours later by CellTiter Blue assay. Bars indicate mean of 6 independent experiments +/- SD. (B) BTC cells were transfected and assessed for CD133+ by FACS. The population of CD133+ cells increased with enforced expression of MIR1249. Bars indicate mean of 3 independent experiments +/- SD. Representative pictures of

the FACS analysis are shown; CD133+ cells are identified by the double positivity of APC-A and GFP-A (right upper quadrant). (C) BTC cells were sorted for CD133 and collected for RNA extraction. Bars represent LOG value of the indicated ratio with the relative control (positive values above the x-axis indicate increase in expression vs relative control). All markers are increased in CD133+ (vs CD133-) cells and after transfection of unsorted cells with MIR1249 mimic (vs mimic control). Bars indicate mean of at least four independent replicates +/- SE. * $p < 0.05$; ** $p < 0.01$; *** $p < 0.001$ vs relative control. (D) CCLP-1 cells were treated with DMSO or CG chemotherapy after transfection with CTRL or MIR1249 inhibitor and assessed for CD133+ by FACS. CG induced enrichment of CD133+ cells, and this enrichment was reduced in case of transfection with MIR1249 inhibitor. Bars represent mean of 3 independent experiments +/- SD. Representative pictures of FACS analysis are shown on the right. Pink dots represent CD133+ cells. (E) WT and MIR1249KO CCLP-1 cells were treated with DMSO and CG chemotherapy at scalar doses up to 5M cisplatin and 50nM gemcitabine. Bars represent the log of the ratio between CG- and DMSO-treated cells. Bars indicate mean of 6 independent experiments +/- SD. (F) WT and 2 clones of MIR1249KO cells were treated with DMSO and CG chemotherapy and assessed for CD133 expression by FACS. Bars represent mean of three independent experiments +/- SD. (G) Cells were transfected with CTRL mimic or MIR1249 mimic and treated with DMSO and CG chemotherapy. Bars represent mean of 6 independent experiments +/- SD. *** $p < 0.001$ (see also Figure S3).

Figure 5. MIR1249 activates the Wnt pathway by acting on FZD8. (A) CCLP-1 cells were sorted for CD133 expression and processed for western blotting analysis (left side). CD133- cells were also transfected with the indicated probes for 48 hours before proceeding to western blotting (right side). (B) CCLP-1 cells were sorted and transfected with NFAT and TOP-FLASH vector for 48 hours before luciferase activity was recorded. Bars indicate mean of 6 independent experiments +/- SD. Two-way anova test <0.05. (C) BTC cells were transfected with pMIR-3UTR-FZD8 vector +/- MIR1249 mimic and luciferase activity recorded. Bars indicate mean of 6 independent experiments +/- SD. (D) BTC cells were transfected for 48 hours and positivity for CD133 assessed by FACS. Bars represent mean of three independent experiments +/- SD. (E) CCLP-1 (left) and TFK-1 (right) cells were transfected with siFZD8 or siCTRL for 48 hours and collected for mRNA expression by Taqman. Bars represent log value of the ratio between siFZD8 and siCTRL. Bars indicate mean of three independent experiments +/- SD. * $p < 0.05$; ** $p < 0.01$; *** $p < 0.001$. (F) CG-treated BTC cells were transfected for 48 hours and positivity for CD133 assessed by FACS. Bars represent mean of three independent experiments +/- SD. (G) CCLP-1

cells were infected with the indicated vectors and treated with CG chemotherapy before being fixed in formalin and embedded in paraffin for IHC and ISH (see also Table S4). Scale bars: 100μm. (H) Cells were transfected with NFAT or TOP-FLASH vectors and luciferase activity recorded after 48 hours. CD133+ cells were added as controls. Bars indicate mean of three independent experiments +/- SD. (I) CCLP-1 cells were transfected for 48 hours and treated with DMSO or increasing doses of CG (up to 5uM C and 50nM G). Bars represent the log value of the ratio between CG-treated and DMSO-treated cells. Bars indicate mean of 6 independent experiments +/- SD.

Figure 6. Lack of MIR1249 increases sensitivity to chemotherapy *in-vivo*. (A) WT or MIR1249KO CCLP-1 cells were injected subcutaneously in the flank of NSG mice (N=20 each) and monitored for growth by caliper (see also Figure S4). (B) At day 14 mice were randomized to be treated with a weekly combination of intraperitoneal gemcitabine (150 mg/kg) and cisplatin (2 mg/kg) or vehicle alone for 3 weeks before being sacrificed. Data are presented normalized to baseline pre-treatment tumour size (day 14). Black * indicate p value < 0.05; grey * indicate p value between 0.05 and 0.085 (see also Table S5). (C) Representative pictures of five explanted tumours per group. (D) Explanted tumours of CG-treated were weighted before being stored for analyses. Error bars indicate mean with SE. (E) Mice were weighted periodically over the course of treatment. Bars represent mean of 10 mice +/- SD. * $p < 0.05$. (F) Representative pictures of MIR1249 ISH staining and IHC staining for the indicated proteins performed on the explanted tumours, along with quantitative analysis. Scale bars: 100μM. Three mice per group were analyzed (for a total of 12) and CG- and vehicle-treated tumours were grouped to assess the differences between KO and WT.

Author contribution

Study concept and design (CB); acquisition of data (PC, SH, MF, AL, VG, CV, MG, FT, ISH, RTP MS, VG, SV, GV, JCH); analysis and interpretation of data (PC, CB); drafting of the manuscript (PC); critical revision of the manuscript for important intellectual content (CB); statistical analysis (LC, CB); material support (VC, AS, DC, DA, NV, LB, RG, SJF, MR, UC, RB, ES, VM, DC, LR, AS, PC, VK), obtained funding (CB, NV, PW).

Acknowledgment

Chiara Braconi is recipient of a Lord Kelvin Adam Smith readership from the University of Glasgow. She was the recipient of an Institute of Cancer Research Clinician Scientist Fellowship, a Marie Curie Career Integration Grant from the European Union, an Early Diagnosis Award from Pancreatic Cancer Action and a NIHR Royal Marsden/ICR Biomedical Research Centre project grant. Nicola Valeri is a recipient of a CRUK Career Development Award, a NIHR Royal Marsden/ICR Biomedical Research Centre Flagship Grant, and a Marie Curie Career Integration Grant from the European Union. Aldo Scarpa is a recipient of an Associazione Italiana Ricerca sul Cancro (AIRC) grant n. 12182. We acknowledge Cancer Research UK funding to the Cancer Research UK Cancer Therapeutics Unit at the Institute of Cancer Research. Paul Workman is a Cancer Research UK Life Fellow.

Abbreviations

MIR:microRNA
miRNA:microRNA
BTC:Biliary Tract Cancer
LNA:Locked Nucleic Acid
CG:Cisplatin-Gemcitabine
RNA:Ribonucleic Acid
ISH:in situ hybridization
CRISPR-CAS9:CRISPR-associated protein-9 nuclease
MIR1249KO:MIR1249 Knock Out
DMSO:Dimethyl sulfoxide
WT:wild type

CCA:cholangiocarcinoma
GBC:Gallbladder cancer
RFS:Relapse Free Survival
DMEM:Dulbecco's Modified Eagle Medium
CO2:Carbon dioxide
NOD:non obese diabetic
ARRIVE:Animal Research: Reporting of *In-Vivo* Experiments
AST:Aspartate Aminotransferase
BUN:Blood Urea Nitrogen
SD:standard deviation
GI:growth inhibitory
iCCA:intrahepatic cholangiocarcinoma
eCCA:aextrahepatic cholangiocarcinoma
CTRL:control
ABC:advanced biliary cancers
TCGA:The Cancer Genome Atlas
RAH:Royal Marsden Hospital
BTSC:biliary tract stem cells
CSC:cancer stem cell
FZD8:frizzled class receptor 8
FGFR2:Fibroblast growth factor receptor 2
IDH1:isocitrate dehydrogenase 1
TT:tumour tissue
AT:adjacent tissue
FFPE:Formalin-Fixed Paraffin-Embedded
FACS:Fluorescence-activated cell sorting
ULA:ultra low attachment
APC-A:allophycocyanin axis
GFP-A:*green fluorescent protein axis*
NFAT:Nuclear factor of activated T-cells
IHC:immunohistochemistry

FIGURE 1

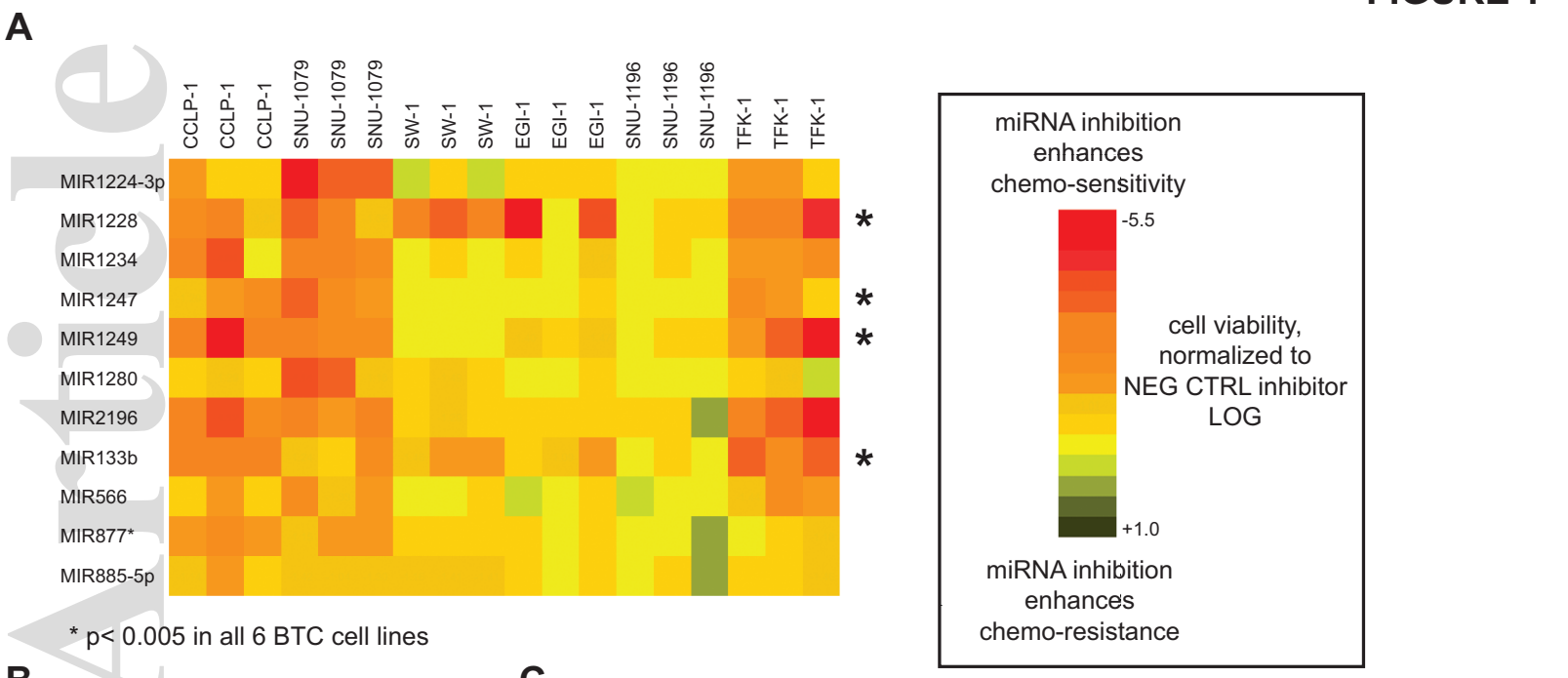

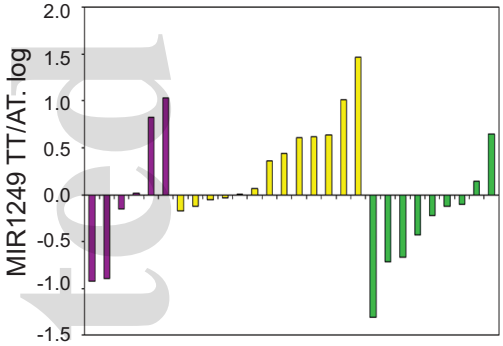

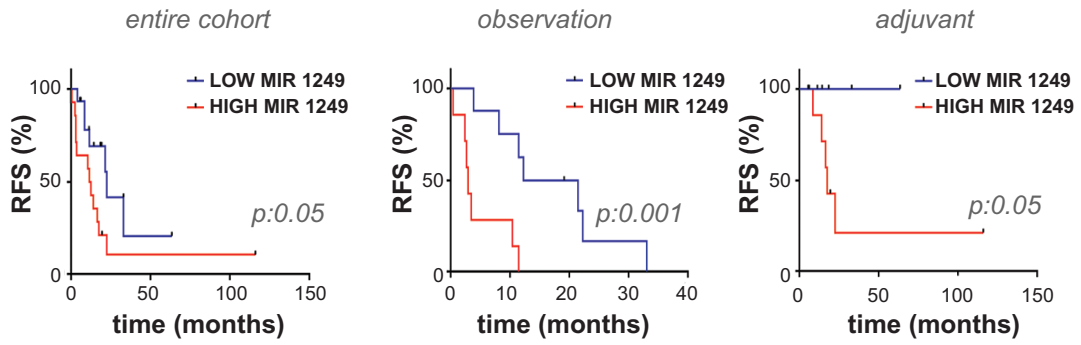

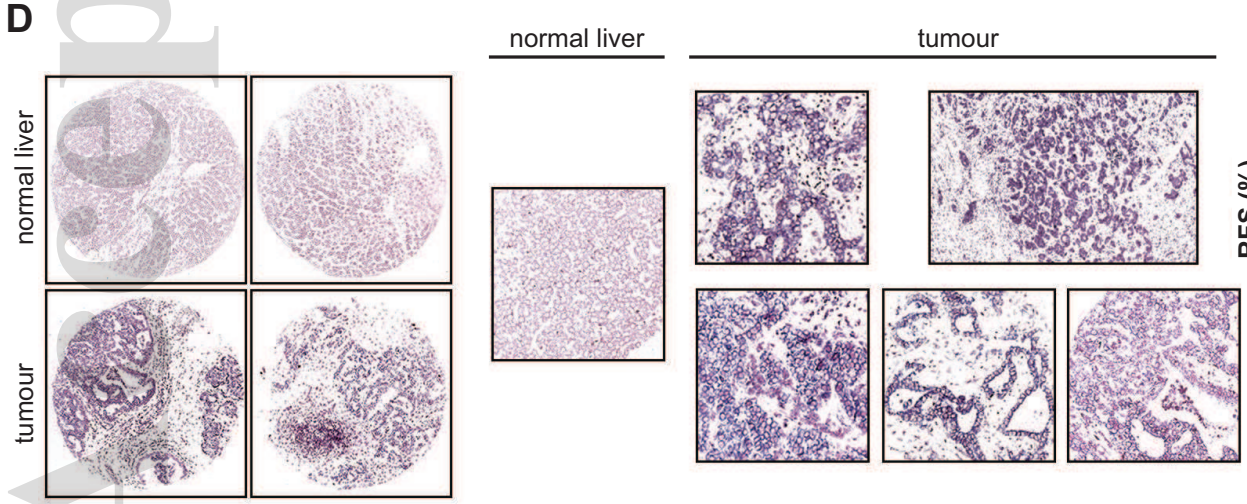

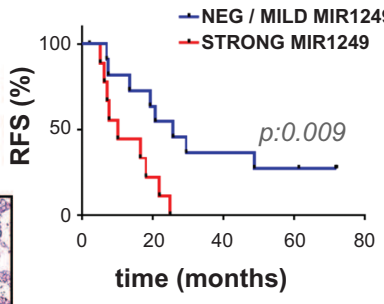

A

FIGURE 2

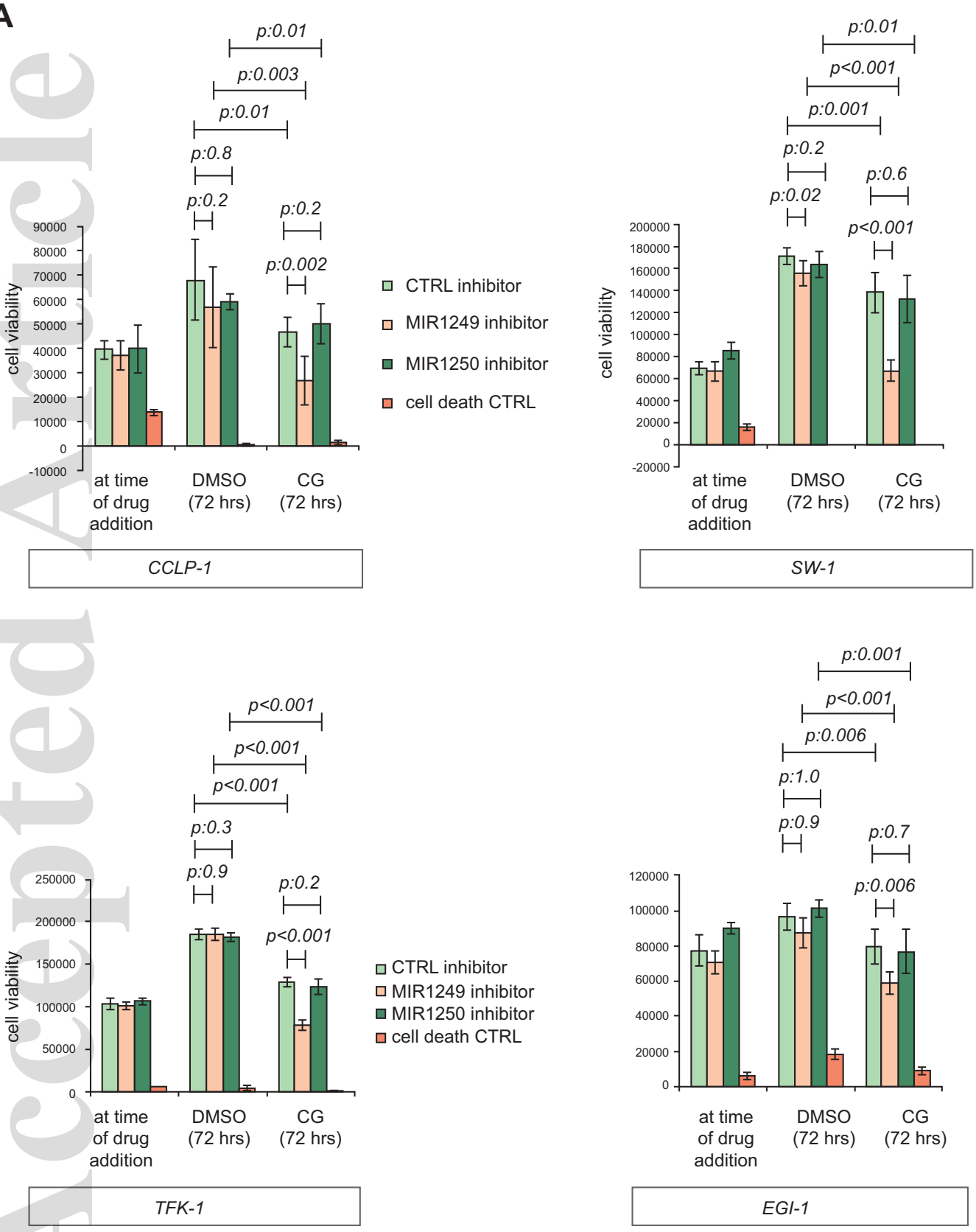

FIGURE 3

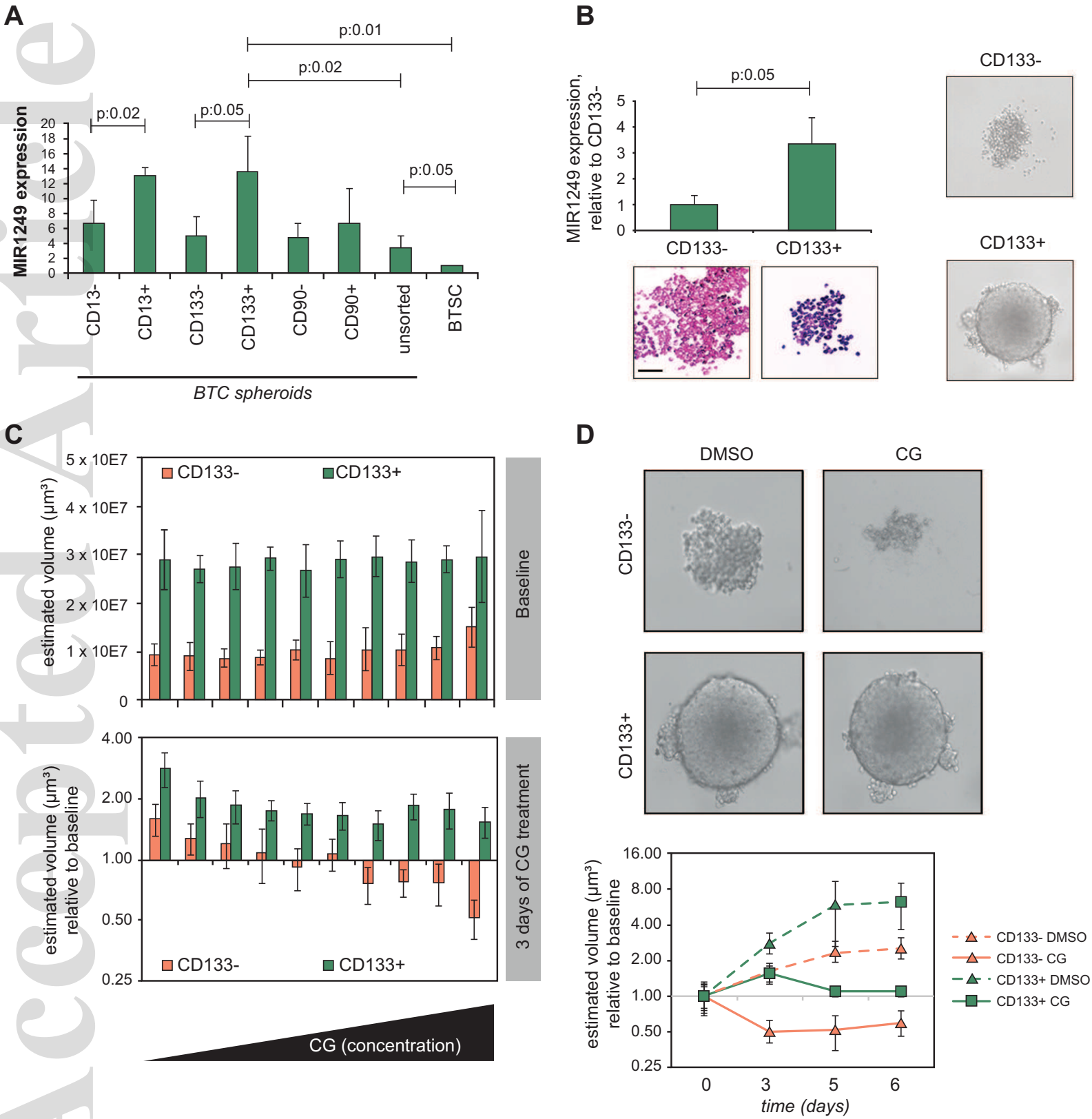

FIGURE 4

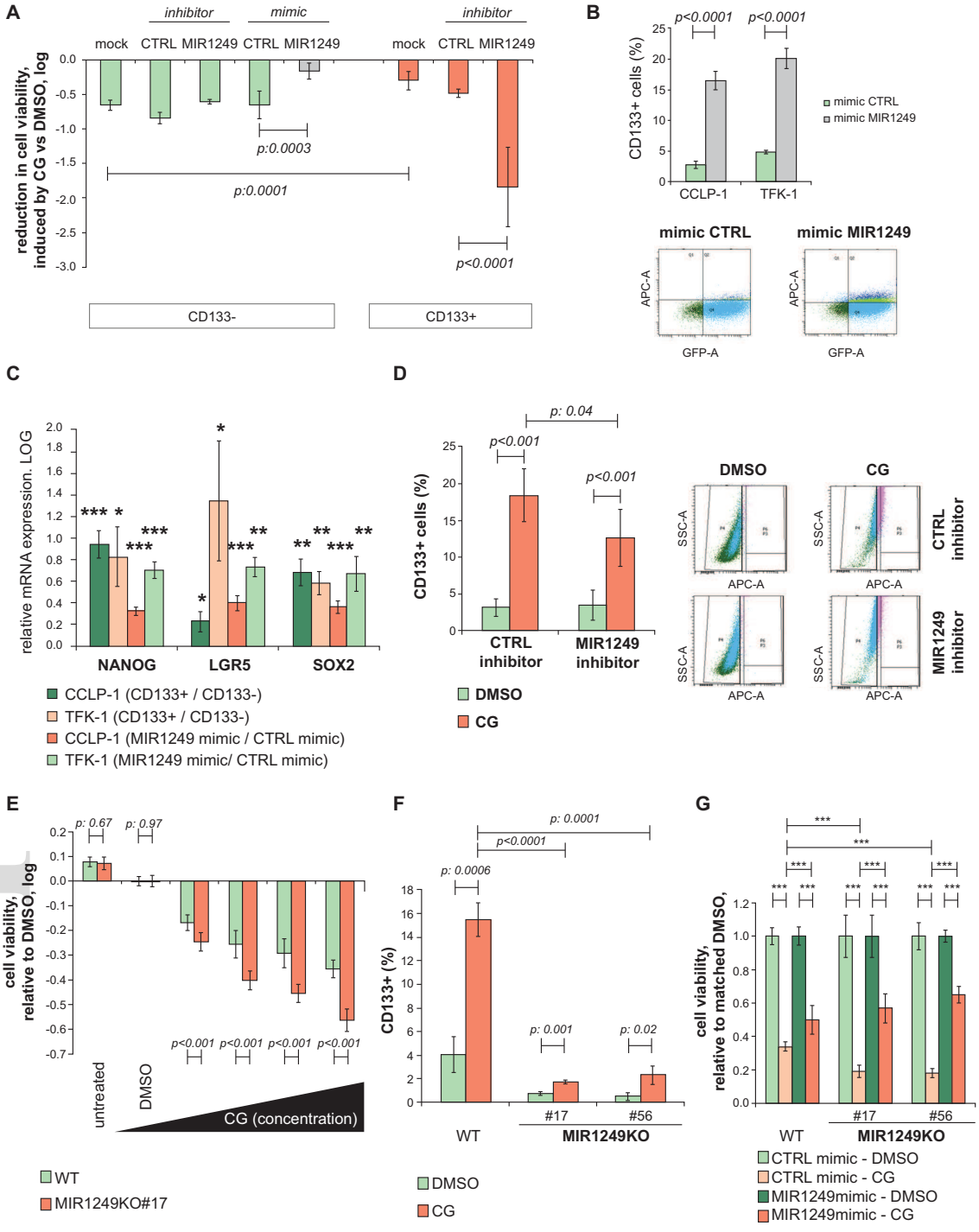

FIGURE 5

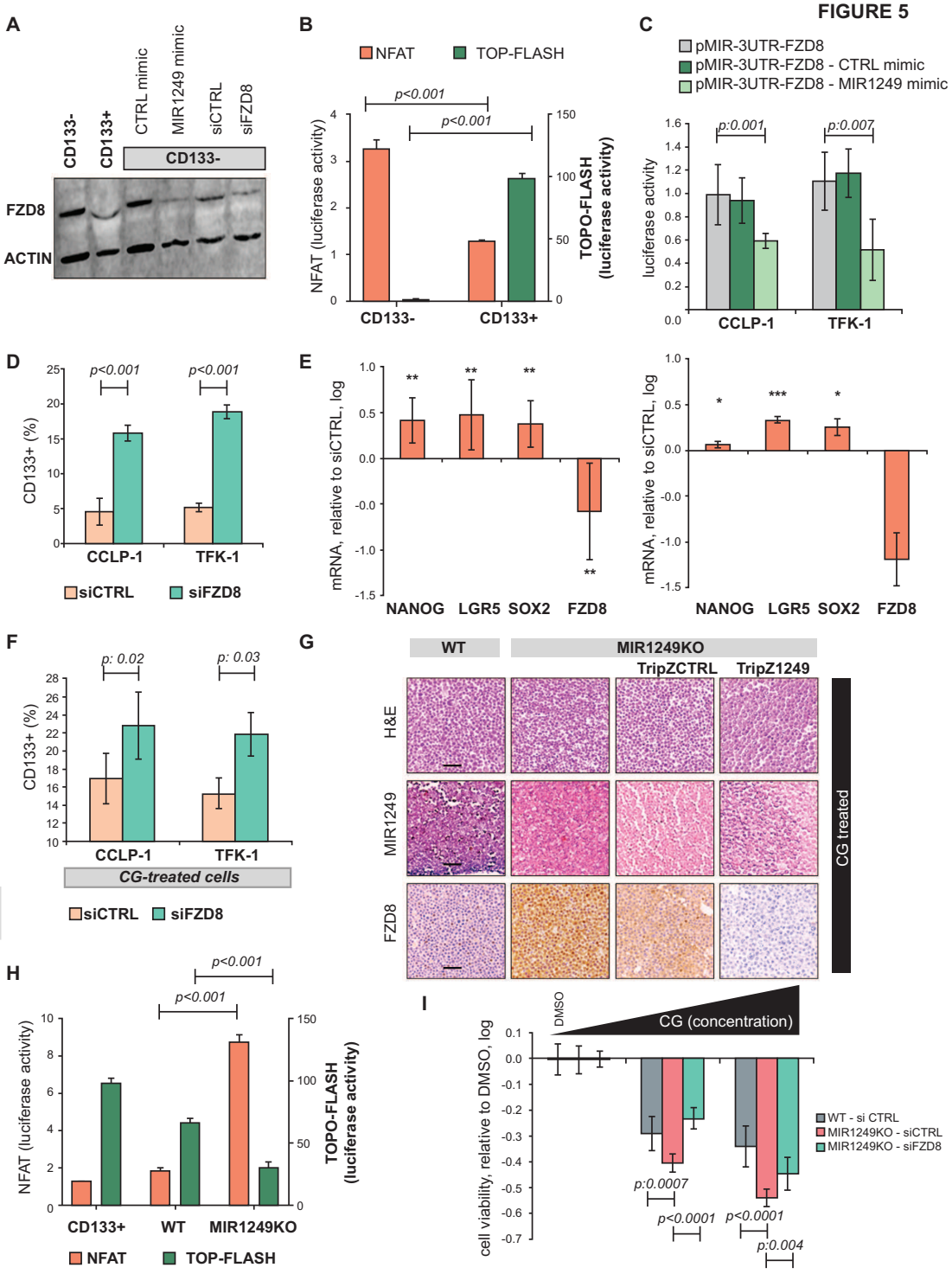

FIGURE 6